

# Leveraging TSP Solver Complementarity via Deep Learning

Kangfei Zhao\*

The Chinese University of Hong Kong  
kfzhao@se.cuhk.edu.hk

Yu Rong

Tencent AI Lab  
yu.rong@hotmail.com

Shengcai Liu\*

University of Science and Technology of China  
liuscyf@mail.ustc.edu.cn

Jeffrey Xu Yu

The Chinese University of Hong Kong  
yu@se.cuhk.edu.hk

## ABSTRACT

The Travelling Salesman Problem (TSP) is a classical NP-hard problem and has broad applications in many disciplines and industries. In a large scale location-based services system, users issue TSP queries concurrently, where a TSP query is a TSP instance with  $n$  points. In the literature, many advanced TSP solvers are developed to find high-quality solutions. Such solvers can solve some TSP instances efficiently but may take an extremely long time for some other instances. Due to the diversity of TSP instances, it is well-known that there exists no universal best solver dominating all other solvers on all possible TSP instances. To solve TSP efficiently, in addition to developing new TSP solvers, it needs to find a per-instance solver for each TSP instance, which is known as the TSP solver selection problem. In this paper, for the first time, we propose a deep learning framework, CTS, for TSP solver selection in an end-to-end manner. Specifically, CTS exploits deep convolutional neural networks to extract informative features from TSP instances and involves data argumentation strategies to handle the scarcity of labeled TSP instances. Moreover, to support large scale TSP solver selection, we construct a challenging TSP benchmark dataset with 6,000 instances, which is known as the largest TSP benchmark. Our CTS achieves over  $2\times$  speedup of the average running time, comparing the single best solver, and outperforms the state-of-the-art statistical models.

## 1 INTRODUCTION

The Travelling Salesman Problem (TSP) is a well-known NP-hard combinatorial optimization problem. Given  $n$  cities, it aims to find an optimal tour that traverses each city exactly once with the shortest traveling distance in total. TSP has broad applications in many disciplines and industries, from routing planning in urban computing to circuit layout in chip manufacturing, from DNA sequencing in bioinformatics to telescope scheduling in astronomy. A most commonly studied TSP, the Euclidean TSP, supposes the cities are in an Euclidean plane (e.g., 2-dimensional space) and the distance between two cities is Euclidean distance. The Euclidean TSP has been widely used in location-based services systems, e.g., satellite navigation systems, and logistics management systems. In such large scale location-based services systems, a large number of users issue TSP queries to pursue near-optimal solutions, where a TSP query is a TSP instance with  $n$  points. Improving the performance for these systems to respond to TSP queries has great significance.

In the literature, many exact and approximate solvers are proposed to solve TSP from the viewpoints of operations research, graph theory, and machine learning. However, like most NP-hard combinatorial optimization and constraint satisfaction problems, different TSP solvers perform best on different TSP instances. It is well recognized that there exists no universal best solver dominating all other solvers on all TSP instances [53, 54]. This fact has incited many researchers to exploit the complementarity between different TSP solvers, by including them into a portfolio. It is expected that an instance would be well solved by at least one solver efficiently. To fulfill this target, there exist two common strategies with a given portfolio of TSP solvers. One is a parallel solver portfolio [14, 17, 33], which runs all TSP solvers independently in parallel until one solves it. The main drawback of this strategy is that it causes a certain waste of computational resources, since running only the best-performing solver on the instance could already achieve the same performance. To resolve such a drawback, one is per-instance solver selection [45], where for each instance, a solver selector selects its best TSP solver from a solver portfolio. The solver selector is built by training data-driven machine learning models offline, with the features and running statistics collected for all the TSP solvers in the portfolio.

However, in the literature, the existing solver selectors suffer from some main drawbacks. First, they all rely on a set of hand-crafted feature set as the synthesis of an input TSP instance (e.g., the distance histogram, the number of clusters and the distance between the centroids based on a clustering algorithm, statistics of the nearest neighbor distances, edge costs of the minimum spanning tree). To obtain high-quality features, a painstaking feature engineering is required to filter redundant, irrelevant and conflict features from a large pool of features. Such feature engineering is time-consuming and sensitive to dataset and model, which means the feature engineering needs redoing once the dataset or model changes. Second, the expressive power of the statistical models used is limited. For fast-growing instance volumes and diversity, the statistical models face the risk of underfitting. In this vein, these motivate us to build an end-to-end deep learning framework for TSP solver selection.

By end-to-end deep learning for a solver selector, it learns the features together with the solver selection task by directly encoding TSP instances into a latent representation using a powerful optimizer (e.g., stochastic gradient descent). In this paper, we construct a Convolutional-based TSP solver Selection (CTS) framework in this end-to-end fashion. Specifically, CTS takes advantage of the

\* Contributed equally.

convolution operator to automatically extract features from a 2-dimensional plane, which is the density map of points for a TSP instance. The deep convolutional neural network has sufficient expressive power to capture spatial patterns related to the performance of solvers from local to global spatial density layer by layer. Furthermore, to handle the scarcity of labeled TSP instances and facilitate better generalization, we give safe data augmentation strategies that are specific for the TSP solver selection task.

We highlight our main contributions as follows. First, we investigate several deep learning models and propose an end-to-end TSP solver selector, CTS, to leverage the complementarity of TSP solvers. To the best of our knowledge, this is the first attempt of using deep neural networks for TSP solver selection. In CTS, we also explore different options regarding the representations of TSP instances, loss functions, and data augmentation strategies. The design of CTS considers the target of solver selection and the combinatorial optimization of TSP together, which is different from image processing in nature. Second, to improve the generalization capability of CTS on unseen TSP instances, we generate the largest TSP benchmark consisting of 6,000 TSP instances following 6 different distributions. The diversity of the benchmark lies in several aspects: the topologies of the TSP instances, the coverage of the feature spaces used in the existing approaches, as well as the performance of TSP solvers. Third, we conduct extensive experimental studies to demonstrate the effectiveness of our approach. Compared with the single best solver, CTS is able to achieve over  $2\times$  speedup of the average running time, and surpasses the best statistical baseline. The TSP benchmark and our implementation will be publicly available.

**Roadmap.** In Section 2, we review the related works of automated solver selection. We give the problem statement in Section 3, and present our end-to-end solver selector in Section 4. In Section 5, we outline the process of generating a large TSP benchmark. We report the experimental studies in Section 6 and conclude the paper in Section 7.

## 2 RELATED WORK

**Automated Solver Selection.** Over the last two decades, solver selection has been successfully applied to many computationally hard problems, including boolean satisfiability problems [35, 39, 56], constraint satisfaction programming [6, 52], continuous black-box optimisation [24, 51, 57], mixed integer programming [14, 20], AI planning [11, 47], software testing/design [28, 40, 46] and database query processing [13]. Machine learning techniques have been regarded as the main-streaming approach for automated solver selection, and two strategies, namely classification and regression, are used. Here, classification models directly predict the solver for each instance [35], whereas the regression models first estimate the performance of each solver, then select the one with the best estimated performance [18, 30, 56]. A comprehensive survey can be found in [27].

**Solver Selection for TSP.** As a sub-field of automated solver selection, TSP solver selection has been studied. Kanda et al. [22] studied 4 classifiers to predict the solver to use and studied neural networks to predict the rankings among the solvers [21]. Pihera and Musliu [43] used 5 different classifiers to predict the best-performing solver.

A recent study [23] used both classification and regression strategies to build TSP selectors, and made an in-depth investigation of feature selection on different feature sets. The experiments in [23] show that the learned selectors can leverage the complementarity of state-of-the-art solvers to boost the performance of diversified instances. All of the existing approaches rely on abundant pre-defined features. However, in practice, it does not mean a better selector using more features. If the features are uninformative or noisy, no selection technique is able to make intelligent decisions.

**Deep Learning for Solver Selection.** To alleviate the tedious task of feature engineering, recently there has been growing research interest in applying deep learning approaches to build solver selection systems. [50] utilized a deep neural network to dynamically select a heuristic search algorithm for autonomous agent search in video games. [34] and [49] both utilized a simple CNN to build solver selectors for satisfiability problems (SAT) and domain-independent planning (DIP), respectively. For SAT, [34] reshapes the ASCII code string of an SAT instance directly to a square gray-scale image. For DIP, [49] firstly transforms an instance to a graph, then transforms the graph to a size-variable image, leaving the graph node ordering and the image resizing as open problems. Neither of them takes advantage of the properties of CNN, which extracts spatial features from small blocks by parameter sharing of 2-dimensional convolution. Although the experimental results of [34, 49] are appealing, it is not shown that these approaches can surpass the state-of-the-art baselines. In addition, they do not equip corresponding data augmentation for their solver selection tasks, and therefore the approaches used have limitation to deploy deep neural networks for large-scale instance solving systems.

## 3 PROBLEM STATEMENT

The Travelling Salesman Problem (TSP) is a classic NP-hard problem in combinatorial optimization, which is to minimize the total travelling distance in visiting a set of points  $V = \{v_1, v_2, \dots, v_n\}$ . In this paper, we study TSP in a 2-dimensional space, where the Euclidean distance between two points  $v_i$  and  $v_j$  is given as  $d(v_i, v_j)$ , and we focus on circuit TSP by which the traveling needs to return to the starting point after visiting the last point. Here, let a permutation  $\Pi = (\pi_1, \pi_2, \dots, \pi_n)$  represent a visiting order, where  $\pi_i$  is to visit a point  $v_j \in V$  in the  $i$ -th position. The circuit TSP (or simply TSP here) is to find a permutation  $\Pi$  over  $V$ , where the distance of the circuit TSP by the permutation, denoted as  $D(\Pi)$ , is minimized.

$$D(\Pi) = \sum_{1 \leq i < n} d(\pi_i, \pi_{i+1}) + d(\pi_n, \pi_1) \quad (1)$$

In the following, without loss of generality, we call one set of points  $V$  one TSP instance.

In the literature, many algorithms are proposed to solve TSP in decades. The state-of-the-art approximate TSP solvers include Helsgaun’s Lin-Kernighan Heuristic (LKH), Generic Algorithm with Edge Assembly Crossover (GA-EAX), and Multi-Agent Optimization (MAOS). And there are algorithms proposed that integrate the techniques in LKH, GA-EAX, and MAOS. Such solvers attempt to find the near-optimal solution for a TSP instance. However, it is well-understood that it is impossible to identify one single solver that can find the near-optimal solution in reasonable time for any

possible TSP instances [53, 54]. This fact suggests that, in addition to design and development of new solvers, it also needs to consider how to select one solver among a set of TSP solvers for a TSP instance in a given collection of TSP instances, which is known as TSP solver selection problem.

**The TSP Solver Selection:** Given a set of TSP instances,  $\mathcal{J} = \{I_1, I_2, \dots, I_n\}$ , and a set of TSP solvers  $\mathcal{S} = \{S_1, S_2, \dots, S_m\}$ , the TSP solver selection problem is to find a per-instance mapping  $\mathcal{M} : \mathcal{J} \rightarrow \mathcal{S}$  that minimizes the penalized average running time (PAR) of  $\mathcal{J}$ . Here, the penalized average running time (PAR) [9] is a widely used hybrid performance measure for combinational optimization. In our problem setting, with PAR, a penalty,  $c \cdot T$  is given to a solver  $S_i$ , if  $S_i$  cannot find the optimal answer for  $I_j$  in  $T$  time, where  $T$  is known as cutoff time and  $c$  is a constant (e.g.,  $c = 10$ ). In other words, the max running time for a solver to handle any TSP instance is  $c \cdot T$ . With such  $T$  given, the penalized average running time can be obtained for a solver  $S_i$  to handle  $\mathcal{J}$ . To evaluate the solver selector  $\mathcal{M}$ , as given in the literature, it needs to compare with two baselines, namely, the virtual best solver (VBS) and single best solver (SBS). Here, VBS is the perfect selector which always selects the best solver for each instance in  $\mathcal{J}$  without any selecting cost. The VBS is treated as the upper bound of a solver selector that can achieve ideally. Due to imperfect selection and the overhead, there are no solver selectors that can achieve VBS. On the other hand, SBS is one solver selected from the candidate solver set  $\mathcal{S}$ , which has the minimum penalized average running time over  $\mathcal{J}$ . In real practice, SBS is determined by some algorithm specialists. It requires us to find  $\mathcal{M}$  that outperforms the SBS, by taking the selection cost into consideration. Due to the setting that a solver will terminate when it finds a high-quality solution, we focus on the solvers' efficiency to deal with TSP instances, which is non-trivial. The challenges of finding such a solver selector are two-fold. First, the selector to be found should be able to select an efficient solver for any single TSP instance by leveraging the features hidden in the TSP instance. Second, the selector should be able to balance its selection error to achieve an overall improvement for the entire collection of TSP instances.

## 4 A DEEP LEARNING APPROACH

There are two prevailing models, the graph convolutional network (GCN) [26] and the convolutional neural network (CNN) [29], that can be adopted to learn a TSP solver selector, as the models are designed to handle geometric and spatial data (e.g., TSP data).

We explored both options, and adopt CNN. We explain why GCN does not perform well below. In order to use GCN, a TSP instance needs to be transformed into an edge-weighted complete undirected graph  $G = (V, E)$ . Here, the node set  $V$  is the same set of the points in the TSP instance, and  $E$  is the edge set for all node pairs. The weight of an edge  $(v_i, v_j)$  is the distance between points  $v_i$  and  $v_j$  in the TSP instance. Thereby, solving TSP for the given instance is equivalent to find the shortest Hamilton circuit on  $G$ . This edge-weighted graph,  $G$ , can be directly fed into a message-passing GCN to predict the best solver. However, in practice, GCN is infeasible to serve as a TSP solver selector for several reasons. First, the graph convolution layer is regarded as a special Laplacian smoothing on the node features for new features generation. However, the

points in a TSP instance do not have hands-on features except their coordinates. Second, when the input is a complete graph, GCN degenerates into a graph network variant *Deep Sets* [58]. The over-smoothing problem [31] of GCN will be aggravated as the model aggregates all points. Third, as the time complexity of training a GCN is linear to the number of edges, for most TSP instances that are with hundreds even thousands of points, it is untraceable to train a GCN even through some sampling-based models can reduce the complexity of the complete graph.

### 4.1 A CNN-based Approach

Convolutional Neural Network (CNN) is a well-known deep neural network architecture, which is commonly applied in the field of image processing and computer vision. A typical CNN is generally composed by multiple alternative convolutional layer with non-linearity and the pooling layer, followed by the fully-connected layers. For input data whose layout is a 2-dimensional grid, the convolutional layers extract features from small blocks by shareable weights, i.e., the filters. The pooling layer aggregates the information from local blocks, reducing the representation size and making it to be more learnable, thereby preventing overfitting. The fully-connected layer is used for specific learning task (e.g., image classification, object detection, image segmentation) equipped by the loss criterion. The success of CNN in image data lies in the fact that (i) the convolutional layers preserve the spatial connection between pixels and their neighbors, and (ii) the pooling layers make the convolution process invariant to translation, rotation and shifting. The time complexity of the training and inference by CNN is given in [15]. The total time complexity of all convolutional layers is  $O(\sum_{l=1}^d n_{l-1} \cdot s_l^2 \cdot n_l \cdot m_l^2)$ , where  $n_{l-1}$  is the number of output (input) channels for the  $(l-1)$ -th ( $l$ -th) layer,  $s_l$  and  $m_l$  are the size of the filter and the output feature map of the  $l$ -th layer, respectively.

### 4.2 From TSP Instance to Image

Given a TSP instance of  $n$  points  $\{v_1, v_2, \dots, v_n\}$ , where each point  $v_i$  has its  $(x, y)$  coordinate as  $(v_i.x, v_i.y)$ . The raw coordinates in a TSP instance are re-scaled to an interval  $(0, 1)$  by min-max normalization. As Fig. 1(a) shows, all the points of one TSP instance fall into a  $(0, 1)^2$  square after the normalization. There are two ways to represent a TSP instance in a 2-dimensional map: distance-based and density-based.

By distance-based, for a TSP instance with  $n$  points, a distance map is constructed by an  $n \times n$  matrix  $M$  where  $M(i, j) = d(v_i, v_j)$ . The distance-based is not effective for two main reasons. First,  $M$  becomes different in size for different TSP instances with different  $n$ . Second, an  $n \times n$  matrix  $M$  to be constructed for a given TSP instance with  $n$  points has greatly affected the learning performance. This is because the matrix  $M(i, j)$  constructed implies an order of points. However, the prearranged order among points introduces a spatial-related bias, which greatly influences the learning of CNN. We have explored different ways of constructing a matrix. There does not exist an order among points in constructing a matrix, which can lead better performance.

By density-based, a density map, that preserves the spatial connection among points and does not implies any ordering among points, is constructed as a  $c \times c$  matrix  $M$  by uniformly dividing the

entire  $(0, 1)^2$  square into  $c \times c$  cells where  $M(i, j)$  counts the number of points falling into the  $cell(i, j)$  (Eq.(2)).

$$M(i, j) = |v|, v \in cell(i, j), i, j \in \{1, 2, \dots, c\} \quad (2)$$

Fig. 1(b) shows this discretization transformation when  $c$  is set as 256. It transforms the  $n$  coordinates of continuous value into a fixed size matrix of integer value. After this step, a TSP instance can be learned as a regular image. A potential problem of Fig. 1(b) is that the density map tends to be sparse. About 800 points are scattered in  $256 \times 256$  cells, where almost all cells are empty. To alleviate the sparsity regarding density, we reduce the number of cells by up-scaling the image with neighborhood interpolation. This image enhancement also improves the resolution of the image, which is favourable for CNN to learn features via deep layers. Fig. 1(c) shows up-scaling a  $64 \times 64$  density map by 4 times, resulting in a  $256 \times 256$  image. Compared to Fig. 1(b) of the same size, the up-scaled image is more clear and sharper.

We adopt the density map to represent an TSP instance for the reasons that it maintains the spatial connections among points and it does not depend on any node ordering to be used.

### 4.3 Loss Function Choices

Given  $n$  TSP instances,  $\mathcal{I} = \{I_1, I_2, \dots, I_n\}$ , and  $m$  solvers,  $\mathcal{S} = \{S_1, S_2, \dots, S_m\}$ , the performance for  $m$  solvers to deal with  $n$  instances is represented as  $\mathcal{T} = \{t_1, t_2, \dots, t_n\}$ , where  $t_i \in \mathbb{R}^m$  is an  $m$ -element vector such that  $t_{ij}$  is the running time of solving instance  $I_i$  by solver  $S_j$ . We aim at building a model which maps a TSP instance represented as a density map to its best solver. There are two approaches. One is to treat  $m$  solvers as  $m$  classes with which we train a CNN classifier with  $m$  classes. One is to treat it as a regression problem to train CNN based on the estimated performance of the  $m$  solvers.

Consider to train a CNN classifier with  $m$  classes as to deal with an image classification task. The loss of multi-class classification for one instance  $I_i$  is given in Eq. (3).

$$L_{CE}(I_i) = \sum_{j=1}^m w_{ij} \cdot p_{ij} \cdot \log(q_{ij}) \quad (3)$$

Here,  $p_i \in [0, 1]^m$  is the empirical distribution of selecting the  $m$  solvers for instance  $I_i$ , which can be set as a function of  $t_i$ ;  $q_i \in [0, 1]^m$  is the predicted likelihood of  $I_i$ , which is the output of CNN followed by the softmax function; and  $w_i \in \mathbb{R}^m$  is an optional weight vector of  $I_i$ .

However, the main issue that need to be reconsidered is whether the cross entropy loss (Eq. (3)) is suitable for TSP solver selection. The answer is negative. First, there are TSP instances where multiple solvers perform the similar best. For these instance, setting  $p_i$  to 0-1 hard label for one of them will neglect the other best candidate solvers, while setting  $p_i$  to probabilistic soft label will blur the supervision of the label. Second, it does not meet the objective of the solver selection which is to minimize the penalizing average running time for a collection of TSP instances.

In this work, we also model solver selection as a regression problem. Instead of directly predicting a solver, we build a performance estimator and choose the solver with the best estimated performance. We use the mean square error (MSE) as the loss of the

regressor.

$$L_{MSE}(I_i) = \sum_{j=1}^m w_{ij} \cdot \sqrt{(q_{ij} - t_{ij})^2} \quad (4)$$

In Eq. (4), the output of CNN,  $q_i \in \mathbb{R}^m$  is the estimated performance of the  $m$  solvers on the instance  $I_i$ . Optionally,  $w_i \in \mathbb{R}^m$  is the weight vector regarding to  $I_i$ . The benefit of regression is that it directly leverages the differences of the running time in the learning process.

### 4.4 Data Augmentation for TSP

To train a CNN for TSP density maps, we need a large amount of training data. The more the training data, the better the generation ability the CNN can achieve. We consider using data augmentation for TSP density maps, as a common technique used for images including cropping, rotation, translation, and noise injection [42, 48], to enlarge the data diversity. However, some issues need to be considered on how the data augmentation techniques can be safely applied to TSP solver selection. Here, the safety of data augmentation method refers to its likelihood of preserving the label post-transformation [48]. It is important to note that, different from conventional computer vision tasks, TSP is a combinatorial optimization problem and a solver to be identified is sensitive to local disturbance. In other words, this requests that the data augmentation for the TSP instances strictly preserve the spatial distribution of the original points, in order to make the performance of TSP solvers on the pre-transformed and post-transformed instance consistent. From this viewpoint, the commonly used cropping, translation, and noise-injection are unsafe data augmentation for TSP solver selection. We explain it below. Here, cropping crops a central patch of the image, and translation shifts the image to one direction and fills the remaining pixels to a constant. This implies that some points will be dropped from the TSP density map, which we need to avoid. As for noise injection which injects a matrix of random value drawn from a Gaussian distribution, it will disturb the distribution of the TSP density map, and will affect learning performance. In this work, for TSP solver selection, we use the data augmentation rotation and flipping techniques. Note that: flipping over any straight line is safe for TSP instances, and rotation can be regarded as a kind of lossless translation of TSP instance.

**Flipping:** The easiest flippings are horizontal flipping and vertical flipping, which flip all the coordinates in  $(0, 1)^2$  by line  $x = 0.5$  and  $y = 0.5$ . The flipping of Fig. 1(c) are shown in Fig. 1(d) and Fig. 1(e), respectively. In the figures, we can observe that the flipping brings symmetric images as well as the features, and preserves the labels by keeping the relative position and the distance between all pairs coordinates. There are two ways for flipping. One is to flip the density map and the other is to flip the raw coordinates. We have to flip the raw coordinates instead of density image. This is because the points around the border of  $(0, 1)^2$  could not fall into  $(0, 1)^2$  any more, if we flip an image by any straight line (e.g.,  $y = x$ ). Thus, we perform the flipping on the raw coordinates of a TSP instance followed by the min-max normalization and the gridding.

**Rotation:** Given  $\theta \in (0, 2\pi)$ , the rotation will rotate all coordinates of a TSP instance by degree  $\theta$ . Fig. 1(f) shows the density map which rotates Fig. 1(c) by  $\frac{\pi}{2}$ . Rotation can be regarded as a kind of

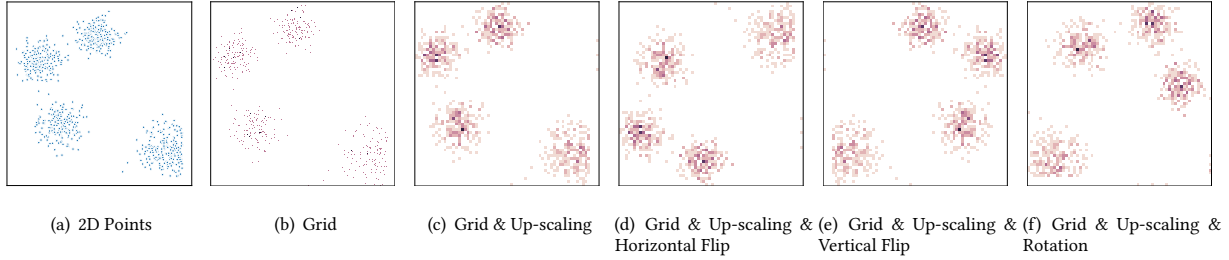


Figure 1: An Example of TSP Data Transformation

lossless ‘translation’ of TSP instance, and is safe for TSP, for any  $\theta \in (0, 2\pi)$ . Similar to flipping, we also conduct rotation on the raw coordinates of the TSP points.

The data augmentation flipping and rotation, essentially only change the appearance of the density map image. They are not image transformation but coordinate transformation, the nature of a TSP instance (i.e., the distance between all pairs points) is intact. Therefore, the CNN filters can still learn the spatial features of different direction symmetrically from any TSP instance. The flipping and rotation are independent, which means one transformation cannot be derived by the other. Therefore, two kinds of flipping and rotation to  $d$  directions can achieve  $2 * d$  extra images for one TSP instance. In the training, the CNN is trained by feeding randomly flipped and rotated density map.

## 5 DATA DESCRIPTION

In this section, we describe the details of the generated benchmark used for building the end-to-end TSP solver selector, which contains 6 TSP solvers, running over 6000 TSP instances of 6 types.

### 5.1 TSP Solvers

For building the TSP solver selector, following [23], we consider three state-of-the-art approximate TSP solvers, i.e., LKH, GA-EAX and MAOS. Due to the rather different approaches underlying them, they are likely to achieve complementary strength in running time across extensive and diversified benchmarks.

**HelsgaunãŽs Lin-Kernighan Heuristic (LKH).** LKH is a variant of the well-known Lin-Kernighan (LK) heuristic [32], which generates local search moves by constructing a sequence of edge exchanges involving five or more edges. In addition, it integrates a multi-restart mechanism that restarts the local search process from new solutions obtained by solution perturbations. Over decades, LKH has been widely recognized as the recommended method for finding high-quality solutions to a large variety of TSP instances.

We use the latest version (2.0.9) of LKH [2]. To deal with the stagnation behaviour of vanilla LKH, [12] enhanced it by triggering the restart mechanism immediately if a better solution is not found in  $n$  iterations, where  $n$  is the number of points of the TSP instance. We implemented this variation as LKH(restart). Moreover, LKH is shipped with a genetic algorithm that uses a genetic operator (i.e., crossover) to generate new solutions as the initial solutions for the local search process. This variation is denoted as LKH(recom).

**Genetic Algorithm with Edge Assembly Crossover (GA-EAX).** Genetic algorithms using variants of edge assembly crossover (EAX) [36, 37] is another successful line of research into solving TSP approximately. Among them, the representative is GA-EAX [38], which integrates an efficient implementation of EAX and additionally includes a local search procedure to generate even better solutions. GA-EAX have matched (and even outperformed) the performance of LKH in finding high-quality solutions to a broad range of Euclidean TSP instances.

As some runs of GA-EAX would be terminated prematurely [12], we modified the solver to perform restart whenever its original termination criterion is met, and to terminate only when it finds a solution with given quality or a given time budget is exhausted. We denote this variation as GA-EAX (restart).

**Multi-Agent Optimization (MAOS).** MAOS [3, 55] is a multi-agent based TSP solver which does not contain any explicit local search heuristic. During the optimization, each agent has only limited knowledge of the TSP instance and explore possible solutions in parallel. Based on the results in [55], the performance of MAOS is competitive with the original versions of LKH and GA-EAX on some TSP benchmarks. We modified MAOS to terminate when reaching a given solution quality or exhausting a given time budget. Following [55], we set the number of agents to 300.

In summary, this paper considers 6 TSP solvers in total, i.e., LKH, LKH(restart), LKH(recom), GA-EAX, GA-EAX (restart), and MAOS. It is worth mentioning that the design of CTS is independent to the candidate solver set. Thereby, it is flexible to plug new solvers into CTS.

### 5.2 TSP Instances

To fully exploit the power of a solver selection system [45], a diverse set of benchmark TSP instances is requisite. Here, diversity is relevant regarding three aspects [10]. First, the instances should be discriminating enough to test solver performance otherwise there is nothing meaningful that will be learned from the data. Second, for traditional feature-based solver selection approaches, instances should also map to different regions in the feature space such that sub-classes of instances could be modeled. Third, instances with diverse topologies intuitively are more likely to represent problems that also occur in real-world applications. To obtain a diverse set of instances, we collect six different TSP generators from the literature. Among them, one is ‘classical’ and has been used to create test beds for the 8th DIMACS Implementation Challenge [19], while the other five are proposed by a recent study [10] in which they have

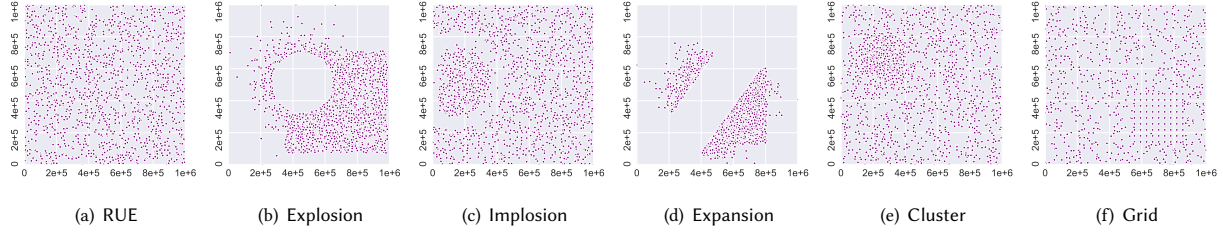


Figure 2: 6 types of TSP instance

been shown to be effective to generate TSP instances with highly desirable diversity properties. Fig. 2 gives illustrations of different types of instances, from which one could identify significant differences between them. In the following, we give a brief overview of the 6 types of TSP instances we used.

**RUE Instances** (Fig. 2(a)). The random uniform Euclidean (RUE) instance, probably the most widely studied TSP instance type, is obtained by placing uniformly at random  $n$  points in a  $10^6 \times 10^6$  square.

**Explosion Instances** (Fig. 2(b)). The “explosion” is meant to tear holes into the point cloud, which is achieved by simulating a random explosion in the  $n$  points of an RUE instance. All points within the explosion range are pushed out of the explosion area.

**Implosion Instances** (Fig. 2(c)). The “implosion” is the inversion of the explosion, which is achieved by simulating a random implosion in the  $n$  points of an RUE instance. All points within the implosion region are shifting towards the implosion center.

**Expansion Instances** (Fig. 2(d)). Based on an RUE instance, an “expansion” instance is obtained by placing a tube around a linear function and all points within that tube are (orthogonally) pushed out of that region.

**Cluster Instances** (Fig. 2(e)). The “cluster” is meant to introduce dense clusters of points into an RUE instance. First, a cluster centroid is uniformly random sampled, then a set of points are selected at random and are moved into the cluster region.

**Grid Instances** (Fig. 2(f)). Based on an RUE instance, a “grid” instance is obtained by relocating a randomly selected “box” points to a new random location with a regular quadratic grid.

### 5.3 Generating Data

For the above 6 types TSP, we created 6000 instances in total, specifically, 1000 per type. We used the portgen generator from the 8th DIMACS Implementation Challenge [1] to generate RUE and used the corresponding mutation functions in the R-package tspgen [5] to generate the other 5 types of instances. For each instance, the number of points was sampled uniformly from [500, 2000]. For the Cluster instances, the number of clusters was set to 4, 5, 6, 7, 8, for each of which 200 instances were generated. It is worth mentioning that this is the largest TSP instance set ever considered in the literature of TSP solver selection.

Since all the 6 solvers are randomized, we assessed their performance based on five independent runs on each of the 6000 instances. Each run is terminated as soon as the solver finding the optimal

Table 1: Solver Performance

TSP set	Measure	GA-EAX	GA-EAX (restart)	LKH	LKH (restart)	LKH (recom)	MAOS	VBS
RUE	Unique	188	153	204	127	223	81	1000
	Shared	2	2	21	9	16	0	0
	Failed	254	1	11	10	9	6	0
	PAR10	2298.48	36.92	143.47	134.71	126.28	95.62	14.85
Explosion	Unique	220	162	233	99	215	48	1000
	Shared	4	4	17	3	18	0	0
	Failed	194	1	5	3	3	5	0
	PAR10	1758.07	30.14	84.72	66.89	65.73	77.50	12.72
Implosion	Unique	215	152	238	106	199	49	1000
	Shared	6	6	31	6	33	0	0
	Failed	193	1	10	10	11	4	0
	PAR10	1748.04	29.71	129.43	129.29	137.70	71.89	12.60
Expansion	Unique	299	214	10	9	8	451	1000
	Shared	8	8	0	1	1	0	0
	Failed	507	42	316	318	319	11	0
	PAR10	4569.26	432.91	3001.87	3019.59	3026.38	123.02	19.67
Cluster	Unique	239	191	184	83	177	90	1000
	Shared	6	6	24	9	27	0	0
	Failed	246	1	54	55	53	7	0
	PAR10	2225.21	34.35	546.62	555.76	541.13	100.63	14.51
Grid	Unique	189	127	242	93	278	44	1000
	Shared	4	4	20	5	21	0	0
	Failed	234	1	15	13	14	34	0
	PAR10	2117.78	43.78	177.67	160.81	168.64	364.00	15.28
Total	Unique	1350	999	1111	517	1100	763	6000
	Shared	30	30	113	33	116	0	0
	Failed	1628	47	411	409	409	67	0
	PAR10	2452.81	101.30	680.63	677.84	677.64	138.78	14.94

solution<sup>1</sup> or the solver running for a cutoff time of 900 seconds; in the first case, the run is considered successful and in the second case, unsuccessful. The running time of each unsuccessful run is recorded as  $10 \times 900s = 9000s$ . After repeating five independent runs, the median running time over these runs is recorded as the running time on the instance. The aggregated running time of a solver on the instance set is the average of its running time on all instances in the set, which is the widely used PAR10 score [9] with a penalisation factor 10. To build a solver selector, the 6000 instances were split into 4200 instances for training and 1800 for testing, which were stratified split based on the partitions of the instances’ best solver.

<sup>1</sup>The optimal solutions of instances are precomputed by Concorde [7] (<http://www.math.uwaterloo.ca/tsp/concorde.html>), an exact TSP solver.



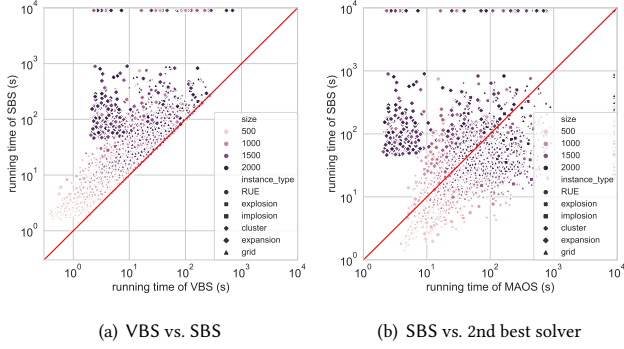


Figure 3: Scatter plots of the aggregated running times of the 6000 instances

**Exploratory Data Analysis.** Table 1 shows the performance statistics of above 6 types instances over the 6 solvers. For each type of TSP instance, We distinguish the number of instances that one solver was the unique solver that performs best and that of the multiple solvers achieve the same best performance, indicated as Unique and Shared in Table 1, respectively. In addition, the number of instances that are failed to find the optimal solution in the cutoff time is denoted as Failed. In general, LKH and its variation LKH (recom) have the top number of unique best on Grid, RUE, Explosion and Implosion and share the best performance on a small fraction of instances. The solver GA-EAX achieves the most unique best on all the 6000 instances. Unfortunately, it also has the largest number of failed instances, leading to the worst PAR10. For GA-EAX (restart), although its performance is not the universal best on all the types of TSP, thanks to the limited number of failed instances, it achieves the minimum PAR10. Thereby, GA-EAX (restart) will serve as the SBS for our following study. It is interesting to find that the restart mechanism plays an important role in boosting GA-EAX, whereas it does not benefit much for LKH. Only a small fraction of instances, 763 in 6000, on which MAOS performs best, and more than half of these instances are from Expansion. But the balanced performance of MAOS makes it becomes the 2nd best solver. Fig. 3 presents a fine-grind comparison of VBS with SBS (GA-EAX (restart)), and SBS with the 2nd best solver (MAOS). As Fig. 3(a) shows, there is a substantial performance gap between SBS and VBS across all instances types and sizes, which solver selection can be used to deal with. Fig. 3(b) compares the SBS with MAOS over all the TSP instances. Among the 6000 instances, MAOS outperforms the SBS on 1145 instances, where 464 are from Expansion. Also, there are a small collection of instances in the other 5 types of instances that MAOS performs better.

## 6 EXPERIMENTAL STUDIES

In this section, we present our experimental evaluations. First, we give the specific setting of the testing. Then, we compare our end-to-end solver selector with the state-of-the-art baselines and the SBS and conduct an ablation study for the data augmentation.

### 6.1 Experimental Setup

**6.1.1 CTS Settings.** Our CTS is built on PyTorch 1.3.1 [4] with Python 3.7. We used Adam [25] optimizer with a learning rate

Table 2: The Hyper-parameter Configuration

Hyper-parameters		Values
CNN	learning rate	$10^{-3} \sim 10^{-4}$
	mini-batch size	{32, 64}
	# epochs	{50, 100}
	lr decay rate	0.9
	lr decay patience	10
Data Transformation	# grid c	64
	Interpolation factor	4
	Random Flip	True
	# Random Rotation in $[0, 2\pi)$	{7, 17}
MLP	# hidden units	{128, 256}
	learning rate	$10^{-3} \sim 10^{-4}$
	mini-batch size	{32, 64}
	# epochs	50
	lr decay rate	0.9
	lr decay patience	10

Table 3: Statistics of the Feature Sets

Feature Set	# Features	Computing Time (s)		
		Median	Mean	Stan. Dev.
UBC [18]	49	9.00	11.74	8.66
UBC-cheap [18]	12	0.12	0.14	1.00
Phiera [43]	287	0.07	0.073	0.04

decay to train the CNN. For the model, we used a state-of-the-art deep CNN, the residual networks (*ResNet*) [16], including the ResNet18 and ResNet34. Equipped with the basic  $3 \times 3$  filters as a shortcut connection, ResNet18 and ResNet34 have 18 and 34 layers, respectively. For the loss function, we used the cross entropy loss (Eq. (3)) for classification, and the mean square error (Eq. (4)) for regression. For the weight  $w_{ij}$  in Eq. (3) and Eq. (4), it was set to  $t_{ij}^\alpha$ , where  $\alpha$  is a tunable penalty factor in  $[0, 1]$ . Table 2 shows the hyper-parameters settings in the training. In the testing phase, the data augmentations, i.e., random rotation and random flip were disabled. Both training and testing were performed on a single Nvidia V100.

**6.1.2 Statistical Models Settings.** We compared our CNN model against the state-of-the-art statistical models for TSP solver selection [23]. Specifically, we repeated the same settings in [23], i.e., 3 learning strategies, 3 statistical models, 4 feature sets, and 2 feature selection approaches, resulting in 72 selectors trained in total. It is worth mentioning that the overall training and feature engineering take one week on an Intel Xeon E5-2699A v4 machine with 44 cores and 256GB RAM. In the following, we elaborate on these settings.

**Learning Strategies.** Apart from classification (Cla.) and regression (Reg.), on the basis of [23], we also adopted pairwise regression (P-Reg.) strategy to train a model which predicts the performance difference between each pair of solvers, resulting in a total of 15 models for one selector. Afterward, the solver with the best predicted performance difference to all the other solvers on the given instance is chosen.

**Models.** The statistical models were built by Python scikit-learn [41]. For each learning strategy, we trained decision trees (DT), random forests (RF), and support vector machines (SVM). Following the setting of [23], each of the models kept its default setting.

**Feature sets.** Table 3 lists the statistics of the feature sets, which were fed into the statistical models isolated and combined. UBC [18]

includes spatial distribution of the points in the Euclidean plane, the distribution of the points distances, degree and edge costs characteristics of a minimum spanning tree as well as some features computed from multiple runs of LKH. UBC-cheap is a subset of 12 computationally cheap features from UBC. Phiera [43], includes a small collection of UBC features as well as some additional geometric features, local search probing features and features based on the k-nearest-neighbor (k-NN) graph of the TSP instance. Finally, we also considered the union set of UBC and Phiera, which has 336 features.

**Feature selection.** Following [23], two different feature selection approaches, namely sequential floating forward search (SFFS) and sequential floating backward search (SBFS), were conducted on each of the 36 solver selectors, i.e., 3 learning strategies  $\times$  3 models  $\times$  4 feature sets, mentioned above. Starting from an empty feature set, SFFS greedily adds one feature at a time based on the selector performance, and would exclude a feature from the set if the exclusion could lead to performance improvement. SBFS is the inversion of SFFS in that it starts from the full feature set by removing one feature at a time based on the selector performance. Both SFFS and SBFS will terminate if neither adding nor dropping any single feature leads to any improvement in selector performance. These two approaches were implemented by Python MLxtend [44]. During feature selection, 5-fold cross-validation was used to assess the performance of the models, based on PAR10 plus the feature computation time. The computation of many features within each feature sets is deeply intertwined; therefore, the computation time of any selected subset is regarded as the entire feature set.

**6.1.3 Multilayer Perceptron Settings.** In addition, we trained two-layer Multilayer Perceptron (MLP) as the neural network baselines. The input of MLP was the 336 dimensional union feature set of UBC and Phiera. Similar to CTS, they also adopted the cross entropy loss (Eq. (3)) for multi-class classification and the mean square error (Eq. (4)) for regression and were trained by Adam optimizer. Table 2 lists the training settings of MLP.

## 6.2 Results and Analysis

Table 4 summarises the overall performance of the statistical models, MLP and the *ResNet* of CTS. Due to the limited space, here for each learning strategy, Table 4 only lists the top-3 statistical models regarding the test PAR10. The feature set of all the 9 models are searched by SFFS. For all the feature-based selectors (i.e., DT, RF, SVM and MLP), the performance on a given TSP instance is the running time of the solver selected plus the computing time of the required feature set. Compared to the solver running time and feature computation time, the model prediction time is negligible. Averaged on each instance, model prediction of CTS spends about  $10^{-3}$  second on CPU and  $10^{-4}$  second on GPU. And the statistical models are MLP need  $10^{-3}$ - $10^{-7}$  second, depending on the model, learning strategy the number of used features. Meanwhile, we list the average rank of the selected solver (Avg. Rank), the percentage of performance improvement (Improv.) and unregress (Unreg.) compared with SBS in all the test instances. Note that there is no strict correlation between PAR10 and Avg. Rank (neither Improv., Unreg). PAR10 involves the discrepancy of solvers' running time

**Table 4: The Performance of Baselines and CTS**

Learn. Stra.	Selector Characteristics		Performance			
	Model	Feat. Set / #Used Feat.	PAR10 (s)	Avg. Rank	Improv. (%)	Unreg. (%)
Reg.	DT	Phiera/4	41.01	3.08	7.50	91.17
Reg.	RF	UBC-cheap/8	58.39	3.05	14.89	85.22
Reg.	SVM	Phiera/3	68.47	3.00	16.72	85.28
Cla.	DT	Phiera/2	145.66	2.95	51.33	51.33
Cla.	SVM	UBC/11	164.64	2.90	53.22	53.22
Cla.	SVM	UBC-cheap/6	392.47	3.02	50.67	50.67
P-Reg.	SVM	UBC-cheap/5	118.35	3.00	49.56	49.56
P-Reg.	SVM	UBC/17	135.38	2.96	50.61	50.61
P-Reg.	DT	Phiera/2	147.05	4.28	17.83	17.83
Reg.	MLP	union/336	52.87	2.17	7.06	88.89
Cla.	MLP	union/336	57.66	2.12	7.22	90.67
Reg.	ResNet18-		<b>38.23</b>	2.30	7.70	80.17
Reg.	ResNet34-		<b>36.89</b>	1.92	18.56	86.83
Cla.	ResNet18-		40.91	2.11	6.70	92.09
Cla.	ResNet34-		45.93	2.04	8.17	93.83
-	SBS	-	97.02	2.09	0.00	100.00
-	VBS	-	13.90	1.00	86.10	100.00

and is more sensitive and timeout cases while Avg. Rank, Improv. and Unreg. reflect a rough selection preference of the selector.

**Different Models.** In general, the selectors of CTS outperform the statistical baselines in both PAR10 and the Avg. Rank of the selected solver. This result validates deep CNN has the capability to extract useful features from the density map of TSP instance. The top baselines Reg. DT (Phiera) and RF (UBC-cheap) have 2 and 3 timeout instances, respectively, while the Reg. ResNet18 and ResNet34 both have only 1 timeout instance. For statistical models, we observe that only a small fraction of the available features are selected by the top models, which indicates a majority of the features are not useful for improving the performance of the solver selector. In fact, in our experiments, we find none of the models using all the 336 features are able to beat the SBS. This also reflects the feature engineering process is essential for hand-crafted feature-based solver selection systems.

**Different Learning Strategies.** Another important observation is that the regression (Reg.) strategy significantly outperforms the classification (Cla.) strategy, and the result is consistent with all the selectors. As our concern in Section 4.3, the classification solely relies on matching the empirical distribution of the best solvers so that the Cla. models tend to achieve relatively higher Avg. Rank and the improvement ratio. But the cross entropy loss does not take the magnitude of the discrepancy of running time into account. The instance-wise weights in Eq. (3) can only alleviate rather than solving this problem. In contrast, regression directly predicts the running time of the solvers, which leveraging more information than classification, especially for the powerful deep learning models, e.g., ResNet18 and ResNet34. The performance of pairwise regression (P-Reg.) models is between Cla. and Reg. models. As one solver selector is composed of 15 statistical models whose prediction is the difference of solvers' running time, we conjecture these introduce more uncertainty and errors in the selector.



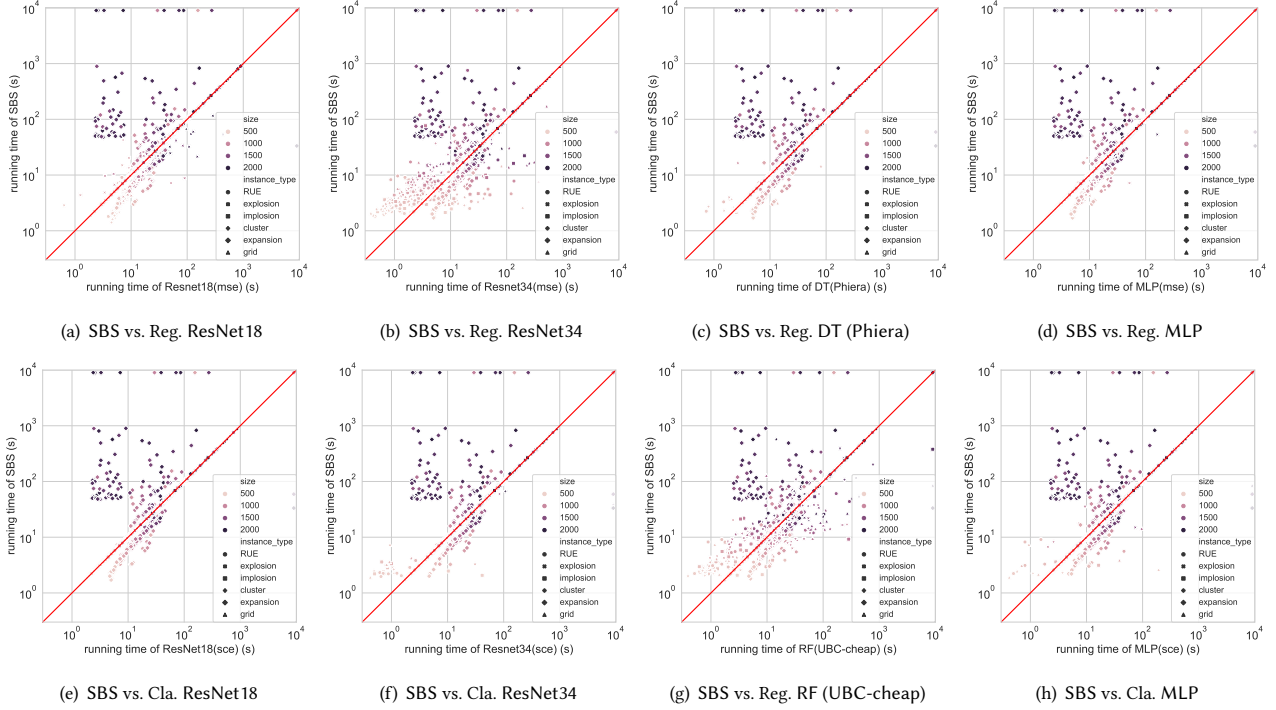


Figure 4: Scatter plots of the aggregated running times of the 1800 test instances

**Selector Visualization.** To make a close observation, we visualize the selection result for several models in Fig. 4, compared with the SBS. Fig. 4(a), 4(b), 4(e), 4(f) are the results for the regression and classification *ResNet* of CTS. Fig. 4(c), 4(g) show the top-2 statistical models, Reg. DT (Phiera) and Reg. RF (UBC-cheap). And Fig. 4(d), 4(h) show the results of Reg. and Cla. MLP. Similar to Fig. 3, the points falling exactly on the red slash line indicate the instances for which the corresponding selector predicts the SBS, i.e., GA-EAX (restart). The instances above the line indicate the selector improves their performance by selecting a better solver with shorter running time, compared with the SBS. And the instances below are those whose performance regress via the solver selection. All the 8 selectors in Fig. 4 attempt to achieve improvement or at least unregress for the large instances with the sacrifice of small instances. That is reasonable for a solver selector to optimize PAR10. For a selector, there is a subtle balance between keeping the choice of SBS and trying to recommend a better solver. The former never incurs performance regress nor improvement while the latter brings the chance of improvement as well as the risk of regress, which is a double-edged sword. In general, most of the models tend to adopt the former conservative strategy, including the classification models and the best statistical baseline Reg. DT with Phiera (Fig. 4(c)). They select SBS for most instances other than Expansion instances. Reg. ResNet18 (Fig. 4(a)) improves some instances of Cluster and Reg. ResNet34 (Fig. 4(b)) can improve all the 6 types of instances. We find a main reason for that is Reg. *ResNet* would select solvers in LKH family for these instances. Their aggressive strategy inevitably leads to prediction error for a small collection of instances. Compared to another aggressive baseline Reg. RF with UBC-cheap (Fig. 4(g)), which 14.78% instances have a performance regress, the

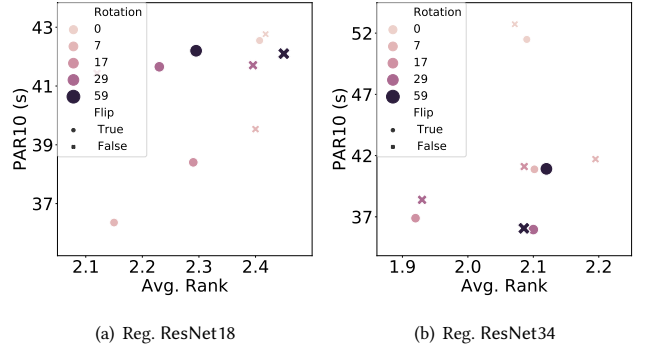


Figure 5: The Effect of Flip and Rotation in CNN Selector

Reg. ResNet34 lead a 13.17% regress ratio. And we observe that for ResNet34, fewer regressed instances are large instances.

### 6.3 Effect of Data Augmentation

We conduct an ablation study to validate the effectiveness of the data augmentation strategies in Section 4. Fig. 5(a) and Fig. 5(b) show the PAR10 and the Avg. Rank of the Reg. *ResNet*, when varying the degree of random rotation with an enabled and disabled random flip. The size and the color of the points indicate the number of directions randomly applied on the TSP coordinates. The dot '•' and the cross '×' indicate the random flip is enabled and disabled, respectively. Except the two augmentations, the models are trained by identical hyper-parameters. First of all, a most important observation from Fig. 5 is that the data augmentations are essential for our task. Since at the top-right of Fig. 5, training without rotation

(i.e., 0 rotation directions) and disabled flipping lead to large PAR10 and low Avg. Rank on the test instances, for both ResNet18 and ResNet34. As we increase the number of rotation directions and turn on the random flipping, the performance of the test result can achieve its best. Compared with ResNet18, ResNet34 trained with more rotation directions will obtain the best performance. That is accordance with our intuition that the larger the model, the more diverse data it required.

## 7 CONCLUSION

It has been demonstrated that different TSP solvers perform best on different TSP instances and this performance complementarity can be leveraged to construct a per-instance TSP solver selector in a large scale TSP solving system. In this paper, for the first time, we provide an end-to-end deep learning framework, CTS, for TSP solver selection. We exploit deep convolutional neural networks to automatically extract features from TSP instances. Our CTS incorporates data enhancement and data augmentation for better generalization. We construct a diversified TSP benchmark set with 6,000 instances, which is known as the largest TSP benchmark. CTS achieves over  $2 \times$  speedup comparing with the single best solver and outperforms the state-of-the-arts statistical models, which may spend days even weeks to obtain the best feature set.

## REFERENCES

- [1] 8th DIMACS Implementation Challenge. <http://dimacs.rutgers.edu/archive/Challenges/TSP/>.
- [2] LKH (2.0.9). <http://webhotel4.ruc.dk/~keld/research/LKH/>.
- [3] MAOS. <https://github.com/wiomax/MAOS-TSP>.
- [4] Pytorch. <https://github.com/pytorch/pytorch>.
- [5] tspgen. <https://github.com/jakobbossek/tspgen>.
- [6] R. Amadini, M. Gabbriellini, and J. Mauro. A multicore tool for constraint solving. In *Proc. of IJCAI'15*, 2015.
- [7] D. Applegate, R. Bixby, V. Chvatal, and W. Cook. Concorde TSP Solver, 2006.
- [8] P. W. Battaglia, J. B. Hamrick, V. Bapst, A. Sanchez-Gonzalez, V. F. Zambaldi, M. Malinowski, A. Tacchetti, D. Raposo, A. Santoro, R. Faulkner, Ç. Gülçehre, H. F. Song, A. J. Ballard, J. Gilmer, G. E. Dahl, A. Vaswani, K. R. Allen, C. Nash, V. Langston, C. Dyer, N. Heess, D. Wierstra, P. Kohli, M. Botvinick, O. Vinyals, Y. Li, and R. Pascanu. Relational inductive biases, deep learning, and graph networks. *CoRR*, abs/1806.01261, 2018.
- [9] B. Bischl, P. Kerschke, L. Kotthoff, M. Lindauer, Y. Malitsky, A. Fréchet, H. H. Hoos, F. Hutter, K. Leyton-Brown, K. Tierney, and J. Vanschoren. Aslib: A benchmark library for algorithm selection. *Artif. Intell.*, 237, 2016.
- [10] J. Bossek, P. Kerschke, A. Neumann, M. Wagner, F. Neumann, and H. Trautmann. Evolving Diverse TSP Instances by Means of Novel and Creative Mutation Operators. In *Proc. FOGA'2019*, 2019.
- [11] I. Cenamor, T. de la Rosa, and F. Fernández. The ibacop planning system: Instance-based configured portfolios. *J. Artif. Intell. Res.*, 56, 2016.
- [12] J. Dubois-Lacoste, H. H. Hoos, and T. Stützle. On the empirical scaling behaviour of state-of-the-art local search algorithms for the euclidean TSP. In *Proc. of GECCO'15*, 2015.
- [13] A. Dutt and J. R. Haritsa. Plan bouquets: A fragrant approach to robust query processing. *ACM Trans. Database Syst.*, 41(2), 2016.
- [14] C. P. Gomes and B. Selman. Algorithm Portfolios. *Artif. Intell.*, 126(1-2), 2001.
- [15] K. He and J. Sun. Convolutional neural networks at constrained time cost. In *Proc. of CVPR'15*, 2015.
- [16] K. He, X. Zhang, S. Ren, and J. Sun. Deep residual learning for image recognition. In *Proc. of CVPR'16*, 2016.
- [17] B. A. Huberman, R. M. Lukose, and T. Hogg. An Economics Approach to Hard Computational Problems. *Science*, 275(5296), 1997.
- [18] F. Hutter, L. Xu, H. H. Hoos, and K. Leyton-Brown. Algorithm Runtime Prediction: Methods & Evaluation. *Artif. Intell.*, 206, 2014.
- [19] D. S. Johnson and L. A. McGeoch. Experimental Analysis of Heuristics for the STSP. In *The Traveling Salesman Problem and Its Variations*. 2007.
- [20] S. Kadioglu, Y. Malitsky, M. Sellmann, and K. Tierney. ISAC - instance-specific algorithm configuration. In *Proc. ECAI'10*, 2010.
- [21] J. Kanda, A. C. P. L. F. de Carvalho, E. R. Hruschka, C. Soares, and P. Brazdil. Meta-learning to select the best meta-heuristic for the traveling salesman problem: A comparison of meta-features. *Neurocomputing*, 205, 2016.
- [22] J. Kanda, A. C. P. de Leon Ferreira de Carvalho, E. R. Hruschka, and C. Soares. Selection of algorithms to solve traveling salesman problems using meta-learning. *Int. J. Hybrid Intell. Syst.*, 8(3), 2011.
- [23] P. Kerschke, L. Kotthoff, J. Bossek, H. H. Hoos, and H. Trautmann. Leveraging TSP Solver Complementarity through Machine Learning. *Evolutionary Computation*, 26(4), 2018.
- [24] P. Kerschke and H. Trautmann. Automated algorithm selection on continuous black-box problems by combining exploratory landscape analysis and machine learning. *Evolutionary Computation*, 27(1), 2019.
- [25] D. P. Kingma and J. Ba. Adam: A method for stochastic optimization. In *Proc. of ICLR'15*, 2015.
- [26] T. N. Kipf and M. Welling. Semi-supervised classification with graph convolutional networks. In *Proc. of ICLR'17*, 2017.
- [27] L. Kotthoff. Algorithm selection for combinatorial search problems: A survey. *AI Magazine*, 35(3), 2014.
- [28] S. Kulkarni, J. Cavazos, C. Wimmer, and D. Simon. Automatic construction of inlining heuristics using machine learning. In *Proc. of CGO'13*, 2013.
- [29] Y. LeCun, K. Kavukcuoglu, and C. Farabet. Convolutional networks and applications in vision. In *Proc. ISCAS'10*, 2010.
- [30] K. Leyton-Brown, E. Nudelman, and Y. Shoham. Empirical Hardness Models: Methodology and A Case Study on Combinatorial Auctions. *J. of the ACM*, 56(4), 2009.
- [31] Q. Li, Z. Han, and X. Wu. Deeper insights into graph convolutional networks for semi-supervised learning. In *Proc. AAAI'18*, 2018.
- [32] S. Lin and B. W. Kernighan. An effective heuristic algorithm for the traveling-salesman problem. *Oper. Res.*, 21(2), 1973.
- [33] S. Liu, K. Tang, and X. Yao. Automatic construction of parallel portfolios via explicit instance grouping. In *Proc. AAAI'19*, 2019.
- [34] A. Loreggia, Y. Malitsky, H. Samulowitz, and V. A. Saraswat. Deep learning for algorithm portfolios. In *Proc. of AAAI'16*, 2016.
- [35] Y. Malitsky, A. Sabharwal, H. Samulowitz, and M. Sellmann. Algorithm portfolios based on cost-sensitive hierarchical clustering. In *Proc. of IJCAI'13*, 2013.
- [36] Y. Nagata. New EAX crossover for large TSP instances. In *Proc. PPSN'06*, 2006.
- [37] Y. Nagata and S. Kobayashi. Edge assembly crossover: A high-power genetic algorithm for the travelling salesman problem. In *Proc. of International Conference on Genetic Algorithms*, 1997.
- [38] Y. Nagata and S. Kobayashi. A Powerful Genetic Algorithm Using Edge Assembly Crossover for the Traveling Salesman Problem. *INFORMS J. on Computing*, 25(2), 2013.
- [39] R. J. Oentaryo, S. D. Handoko, and H. C. Lau. Algorithm selection via ranking. In *Proc. of AAAI'15*, 2015.
- [40] E. Park, J. Cavazos, and M. A. Alvarez. Using graph-based program characterization for predictive modeling. In *Proc. CGO'12*, 2012.
- [41] F. Pedregosa, G. Varoquaux, A. Gramfort, V. Michel, B. Thirion, O. Grisel, M. Blondel, P. Prettenhofer, R. Weiss, V. Dubourg, J. VanderPlas, A. Passos, D. Cournapeau, M. Brucher, M. Perrot, and E. Duchesnay. Scikit-learn: Machine learning in python. *J. Mach. Learn. Res.*, 12, 2011.
- [42] L. Perez and J. Wang. The effectiveness of data augmentation in image classification using deep learning. *CoRR*, abs/1712.04621, 2017.
- [43] J. Pihera and N. Musliu. Application of machine learning to algorithm selection for TSP. In *Proc. of ICTAI'14*, 2014.
- [44] S. Raschka. Mlxtend: Providing machine learning and data science utilities and extensions to python's scientific computing stack. *J. Open Source Software*, 3(24), 2019.
- [45] J. R. Rice. The Algorithm Selection Problem. *Advances in Computers*, 15, 1976.
- [46] R. Sagarna, A. Mendiburu, I. Inza, and J. A. Lozano. Assisting in search heuristics selection through multidimensional supervised classification: A case study on software testing. *Inf. Sci.*, 258, 2014.
- [47] J. Seipp, S. Sievers, M. Helmert, and F. Hutter. Automatic Configuration of Sequential Planning Portfolios. In *Proc. of AAAI'15*, 2015.
- [48] C. Shorten and T. M. Khoshgoftaar. A survey on image data augmentation for deep learning. *J. Big Data*, 6, 2019.
- [49] S. Sievers, M. Katz, S. Sohrabi, H. Samulowitz, and P. Ferber. Deep learning for cost-optimal planning: Task-dependent planner selection. In *Proc. AAAI'2019*, 2019.
- [50] D. Sigurdson and V. Bulitko. Deep learning for real-time heuristic search algorithm selection. In *Proc. AAAI/AIIDE'2017*, 2017.
- [51] K. Tang, F. Peng, G. Chen, and X. Yao. Population-based Algorithm Portfolios with Automated Constituent Algorithms Selection. *Inf. Sci.*, 279, 2014.
- [52] D. Tolpin and S. E. Shimony. Rational deployment of CSP heuristics. In *Proc. of IJCAI'11*, 2011.
- [53] D. H. Wolpert. The supervised learning no-free-lunch theorems. In *Soft Computing and Industry*. 2002.
- [54] D. H. Wolpert and W. G. Macready. No free lunch theorems for optimization. *IEEE Trans. Evolutionary Computation*, 1(1), 1997.
- [55] X. Xie and J. Liu. Multiagent optimization system for solving the traveling salesman problem (TSP). *IEEE Trans. Systems, Man, and Cybernetics, Part B*, 39(2), 2009.

- [56] L. Xu, F. Hutter, H. H. Hoos, and K. Leyton-Brown. SATzilla: Portfolio-based Algorithm Selection for SAT. *J. of Artif. Intell. Res.*, 32, 2008.
- [57] S. Y. Yuen, Y. Lou, and X. Zhang. Selecting evolutionary algorithms for black box design optimization problems. *Soft Computing*, 23(15), 2019.
- [58] M. Zaheer, S. Kottur, S. Ravanbakhsh, B. Póczos, R. R. Salakhutdinov, and A. J. Smola. Deep sets. In *Proc. of NIPS'17*, 2017.